Assessment of the accuracy of local quasigeoid modelling using the GGI method: case study for the area of Poland

MAREK TROJANOWICZ

Institute of Geodesy and Geoinformatics, Wroclaw University of Environmental and Life Sciences, Grunwaldzka 53, 50-357 Wrocław, Poland (marek.trojanowicz@igig.up.wroc.pl)

Received: May 9, 2014; Revised: September 30, 2014; Accepted: May 7, 2015

ABSTRACT

We present results of analyses of the evaluation of the method for local quasigeoid modelling based on the geophysical inversion of gravity data (the GGI method). Relying on precise (with an accuracy level of ± 1 cm) GNSS/levelling height anomalies and surface gravity data, we analysed the method accuracy by a) assessing the accuracy of the model which is based on selected available global geopotential model; b) evaluating the influence of the accuracy of the input data (GNSS/levelling and gravity) on the output model accuracy; and c) analysing the influence of the global model resolution on the quasigeoid model accuracy. Analyses were performed for the area of Poland. As the basic accuracy parameter the standard deviation ($\sigma_{\Delta\zeta}$) of the differences between measured (GNSS/levelling) height anomalies and those established from the model were selected. The results indicate that the accuracy of the quasigeoid output model (in terms of $\sigma_{\Delta\zeta}$) was evaluated at cca ± 1.2 cm irrespective of the global geopotential model used. Such accuracy was also achieved using the global model coefficients only up to the degree $N_{max} = 90$. To achieve the above-mentioned accuracy of the output model, the accuracy of input data should not be lower than cca ± 2.0 cm for GNSS/levelling height anomalies and ± 1.3 mGal for gravity data.

Keywords: local quasigeoid modelling; gravity inversion; geodetic application of geophysical techniques; disturbing potential model

1. INTRODUCTION

The local quasigeoid modelling method based on the geophysical inversion of gravity data (the GGI method) was proposed in *Trojanowicz (2007)*. In the subsequent publication on this method, certain aspects of the proposed solution were clarified and the possibilities of using this approach for areas of different sizes were presented (*Trojanowicz, 2012a*). The optimal values of quantitative parameters of basic input data, like extents of a digital elevation model and the Moho depth model, the extent of the area covered with gravity data and density of gravity data were also estimated (*Trojanowicz, 2015*). The next step in

studying the properties of the discussed approach was to try to evaluate its accuracy, using precise GNSS/levelling data. Due to the availability of relevant data, the area of Poland was selected as the research area. A very large database of gravity data was compiled for this area. In recent years, as part of work related to the integration of the ASG-EUPOS network with the Polish basic horizontal and vertical networks, a network of points with precisely measured GNSS/levelling height anomalies covering the entire country has been determined. The differences calculated at these points, between height anomalies measured and those established from the model, became the basis for assessing the model accuracy. As the basic accuracy parameter, the standard deviation of the differences was selected.

It is worth recalling that for the area of Poland, geoid and quasigeoid models have been regularly developed since the 1960s. Models with an accuracy of a few centimetres have been developed since the 1990s. The first model with such an accuracy was the gravimetric quasigeoid model "quasi95", based on the global geopotential model (GGM) OSU91A (360, 360) and gravity anomalies in a $1' \times 1'$ grid (*Łyszkowicz and Forsberg, 1995*). The model, whose accuracy is estimated at ± 8.7 cm (*Łyszkowicz, 2012*), was fitted to the vertical reference system Kronsztadt 86. In 1996 the Head Office of Geodesy and Cartography made the model available for practical use (*Łyszkowicz, 2012*). The next gravimetric quasigeoid model "quasi97b" (*Łyszkowicz, 2012*) was developed using the FFT technique, based on free-air gravity anomalies in a $1' \times 1'$ grid and the global geopotential model EGM96. The accuracy of the model is estimated at ± 3.6 cm (*Łyszkowicz, 2000*). The "quasi97b" model was used to develop later quasigeoid models - (unpublished) "GEOIDPOL 2001" and (published) "GUGiK 2001" (*Pażus et al., 2002*), with an accuracy estimated at ± 1.8 cm (*Kryński, 2007*). Both models were designed by fitting the "quasi97b" model to the points with measured GNSS/levelling height anomalies. The beginning of the twenty-first century was also a period of intensive research to develop a quasigeoid model with an accuracy of ± 1 cm. This research involved qualitative and quantitative analyses of the data needed to estimate a precise quasigeoid model as well as the quasigeoid modelling methods (*Kryński, 2007*). The result of this work was the development of a series of models described in *Kryński (2007)*. In the following years, new models based on global geopotential model EGM08 (*Pavlis et al., 2012*) were also developed. The most accurate models were the quasigeoid model "GDQ08", developed using gravity data and deflections of the vertical by the least-squares collocation (LSC) method, which was estimated to have an accuracy of ± 1.7 cm (*Kryński and Kloch-Główka, 2009*), and the "quasi09c" model computed from gravity data by the LSC method *(Łyszkowicz, 2010*). The accuracy of the latter model was estimated at ± 1.8 cm (*Łyszkowicz, 2010*) and after fitting the model to the vertical reference system Kronsztadt 86 using LSC, its accuracy increased to ± 1.4 cm (*Łyszkowicz, 2012*). In the study by *Godah et al. (2014)*, a gravimetric quasigeoid model developed by LSC using the GOCE-based GGM TIM-R4 truncated to degree and order 200 was presented. The assessed accuracy of the model ranged from ± 201 cm to ± 3.3 cm, depending on the set of GNSS/levelling test points. On the basis of the same data and using the same method, another quasigeoid model was developed using the EGM08, up to degree 2190. The achieved accuracy ranged from ± 1.9 cm to ± 3.1 cm

(*Godah et al., 2014*) and was comparable to the accuracies of the model using TIM-R4 GGM.

The above-mentioned diversity of geoid and quasigeoid models developed for the area of Poland provides a good background for the analysis contained in this paper.

In this paper the following aspects will be presented: 1) a brief description of the GGI method; 2) the research area and test data; and 3) the results of the calculations.

2. GENERAL DESCRIPTION OF THE GGI METHOD

This paragraph discusses the essence of the GGI method and presents the quantitative requirements for the input data, which need to be satisfied in order to interpret the results of the conducted research correctly. A detailed description of the method may be found in publications by *Trojanowicz (2007, 2012a,b)*.

The GGI method relies on building a local model of disturbing potential which consists of three components (Fig. 1). The first one, denoted as T_Ω, is generated by topographic masses included in volume Ω.

The second component (T_κ) is generated by disturbing masses included in volume κ between the geoid and the compensation surface. Both of the mentioned volumes are limited and go slightly beyond the area covered by the used data. Because the measured input data are also influenced by masses lying outside the volumes Ω and κ, the potential T_r is introduced. This component represents the influence of topographic masses and disturbing masses located outside the volumes Ω and κ. Its role is also to cover systematic and long wavelength errors of the input data. So, for the point *P* located on the terrain surface, the disturbing potential can be recorded as:

$$T_P = T_r + T_\Omega + T_\kappa . \tag{1}$$

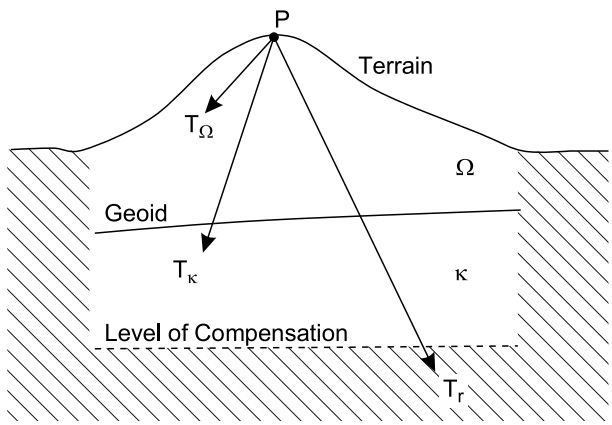

Fig. 1. Components T_Ω, T_κ and T_r of the disturbing potential model.

Components T_Ω and T_κ are calculated using Newton's integrals:

$$T_\Omega = G\iiint_\Omega \frac{\rho}{l} dV_\Omega \ , \tag{2}$$

$$T_\kappa = G\iiint_\kappa \frac{\delta}{l} dV_\kappa \ , \tag{3}$$

where G is Newton's gravitational constant, ρ and δ are density distribution functions for volumes Ω and κ, respectively, dV_Ω and dV_κ are elements of volume and l is the distance between the attracting masses and the attracted point P.

Component T_r describes changes that are of the trend type. It has been represented in all calculations done so far by the following harmonic polynomial:

$$T_r = F\left(X_P, Y_P, H_P\right) = a_1 + a_2 X_P + a_3 Y_P + a_4 X_P Y_P + a_5 H_P \ , \tag{4}$$

where X_P, Y_P are local coordinates of point P and H_P is the normal height of the point.

The model of the disturbing potential defined in Eq. (1) enables us to formulate the following inversion task: to determine such functions of density distribution ρ and δ and polynomial coefficients a_1, a_2, a_3, a_4, a_5 that will satisfy Eq. (1) for the survey data.

The task defined in this way is solved by the discretisation of 3D functions ρ and δ (*Blakely, 1995*). Volumes Ω and κ are thus divided into blocks to which constant density is assigned. The volume Ω is always defined as a regular DEM grid, so it is normal to use such a division to calculate density distribution. Because the determination of density for each DEM block would require finding a large number of unknowns, DEM blocks are connected into zones of constant, searched densities. Volume κ is defined as a plate whose thickness is approximately the same as the depth of the compensation level and consists of one or a few block layers of constant density. In calculations that have been done so far, volumes Ω and κ had the same reach in the horizon plane and the volume κ was presupposed to be a single layer.

Because the solutions of Newton's integrals given by Eqs (2) and (3) are used in calculations, a local Cartesian coordinate system was introduced. The Z axis of the coordinate system is directed towards the geodetic Zenith at the origin point and the X and Y axes lie on the horizon plane and are directed to the north and east, respectively. The origin point of the coordinate system can be set in the middle of the elaboration area.

Given the above, Eqs (2) and (3) can be written as follows:

$$T_\Omega = \sum_{k=1}^{n}\left(\rho_k G \sum_{i=1}^{m_k} \int_{z_{i1}}^{z_{i2}} \int_{y_{i1}}^{y_{i2}} \int_{x_{i1}}^{x_{i2}} \frac{1}{d_i} dx_i \ dy_i \ dz_i \right) , \tag{5}$$

$$T_\kappa = \sum_{j=1}^{s}\left(\delta_j G \int_{z_{j1}}^{z_{j2}} \int_{y_{j1}}^{y_{j2}} \int_{x_{j1}}^{x_{j2}} \frac{1}{d_j} dx_j \ dy_j \ dz_j \right) , \tag{6}$$

where

$$d_i = \sqrt{\left(x_i - X_P\right)^2 + \left(y_i - Y_P\right)^2 + \left(z_i - Z_P\right)^2} \ ,$$

$$d_j = \sqrt{\left(x_j - X_P\right)^2 + \left(y_j - Y_P\right)^2 + \left(z_j - Z_P\right)^2} \ .$$

ρ_k is the searched constant density of zone k, n is the number of DTM zones, m_k is the number of rectangular prisms of DTM in zone k, x_{i1}, x_{i2}, y_{i1}, y_{i2}, z_{i1}, z_{i2} are the coordinates defining the rectangular prism i of DTM, s is the number of rectangular prisms of the volume κ, δ_j is the searched density of rectangular prism j, x_{j1}, x_{j2}, y_{j1}, y_{j2}, z_{j1}, z_{j2} are the coordinates defining rectangular prism j.

The solutions of the integrals occurring in Eqs (5) and (6) as well as the solutions of its derivatives are presented by *Nagy (1966)* and *Nagy et al. (2001)*.

Unknown model parameters (polynomial coefficients a_1, a_2, a_3, a_4, a_5 and densities ρ_k and δ_j) are determined by the least squares method on the basis of the input data, usually in the form of GNSS/levelling height anomalies (converted to the values of disturbing potential in survey points) and gravity data (gravity disturbances or gravity anomalies in survey points). For each measured value, the observation equation is built using Eqs (4)–(6). In matrix notation the system of observation equations becomes:

$$\boldsymbol{v} = \mathbf{A}\boldsymbol{x} - \boldsymbol{L} \ , \tag{7}$$

where: $\boldsymbol{x}^{\mathrm{T}} = \left[a_1, a_2, a_3, a_4, a_5, \rho_1 \ldots \rho_n, \delta_1 \ldots \delta_s\right]$ is the vector of unknowns, $\boldsymbol{v}^{\mathrm{T}} = \left[v_{TP}, \ldots, v_{\delta gP}, \ldots, v_{\Delta gP}, \ldots\right]$ is the vector of adjustment errors, $\boldsymbol{L}^{\mathrm{T}} = \left[T_P, \ldots, \delta gP, \ldots, \Delta gP, \ldots\right]$ is a known observation vector and **A** is the design matrix of known coefficients.

Solution of Eq. (7), using the least square objective function in the form $\min\left(\boldsymbol{v}^{\mathrm{T}}\mathbf{P}\boldsymbol{v} + \boldsymbol{x}^{\mathrm{T}}\mathbf{W}_x\boldsymbol{x}\right)$, is given by the equation:

$$\boldsymbol{x} = \left(\mathbf{A}^{\mathrm{T}}\mathbf{P}\mathbf{A} + \mathbf{W}_x\right)^{-1}\mathbf{A}^{\mathrm{T}}\mathbf{P}\mathbf{L} \ , \tag{8}$$

with

$$\mathbf{W}_x = \begin{bmatrix} \mathbf{W}_a & 0 \\ 0 & \mathbf{W}_\tau \end{bmatrix} ,$$

where **P** is the given weight matrix of observations and, $\mathbf{W}_a$ is the zero model weighting matrix assigned to the vector of polynomial coefficients in Eq. (4), $\mathbf{W}_\tau$ is the weighting matrix of unknown densities whose structure is presented in detail in *Trojanowicz (2012a,b)*. The matrix is formed based on the deep weighting function proposed by *Li and*

Oldenburg (1998). The additional condition $\min\left(\boldsymbol{x}^{\mathrm{T}}\mathbf{W}_x\boldsymbol{x}\right)$ was introduced to the calculations to overcome the non-uniqueness of the gravity inversion (*Li and Oldenburg, 1998*), and it allows control the inversion process to some extent. Global geopotential models and preliminary information on the density distribution in volumes Ω and κ can also be used in calculations. These data are used through the remove-compute-restore (RCR) technique.

Once the model parameters are determined, disturbing potential is calculated using Eqs (4)–(6) in the new points, which in turn is converted to a height anomaly. A more detailed description of the solution is presented in papers by *Trojanowicz (2007, 2012a,b)*.

As was mentioned earlier, there are two kinds of data usually used in the calculations: GNSS/levelling height anomalies and gravity disturbances or gravity anomalies in survey points. The data should cover the entire study area. Our experience suggests that the area covered with gravity data should be larger than the area covered with GNSS/levelling data and volumes Ω and κ should be greater than the area covered with gravity data. Fig. 2 shows the relative location of individual data collection areas. This figure also presents minimal distances between borders of individual groups of data, estimated on the basis of a different research project (*Trojanowicz, 2015*).

The whole area covered with different data may be divided into two parts. The first part constitutes the inner zone whose border is simultaneously the border of the area covered with GNSS/levelling data (shaded area in Fig. 2). This zone defines the area in which we obtain correct modelling results, i.e. where the quasigeoid model is of the highest accuracy. The second part constitutes the outer zone for which the modelling outcomes are considered incorrect.

Points with known GNSS/levelling height anomalies should cover the whole inner zone evenly and the distance between them influences the modelling accuracy - the denser the network, the better the results of the modelling. In research projects conducted so far,

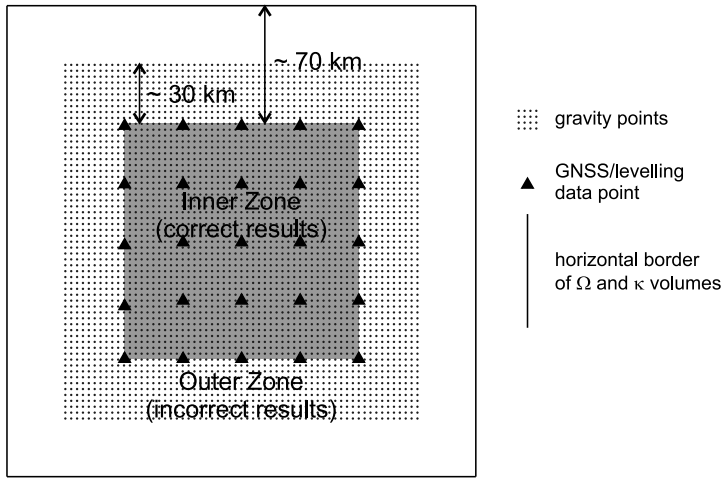

Fig. 2. Relative locations of individual groups of data in a horizontal plane.

high accuracies were achieved when the average distance between points was at a level of 50–70 km. The mean, required density of gravity points was estimated at ca. 1 point per 18 km^2 (*Trojanowicz, 2015*). Since GNSS/levelling height anomalies are used in the calculations, the determined quasigeoid model will always be fitted to the GNSS/levelling data.

3. RESEARCH AREA AND DATA USED IN THE PROJECT

Evaluation of accuracy of the GGI method was based on GNSS/levelling points, the coordinates of which were determined in successive stages of realisation of ITRS and ETRS89 in the area of Poland. Polish part of the EUREF network (EUREF-POL) was formed in 1992. Coordinates of EUREF-POL points were determined in ITRF91 for the epoch of 1992.5 and transformed to EUREF-89 which is an extension of the European reference frame ETRF89 on Polish territory (*Bosy, 2014*; *Zieliński et al., 1993*). This consisted of 11 points network, was densified by POLREF (POLish REference Frame) network (eventually consisting of 348 points). The POLREF network was divided into three sub-networks, which were observed in three campaigns in 1994–1995. Each sub-network was adjusted separately (*Zieliński et al., 1998*). Two of them were solved in ITRF92, each for different epochs: 1994.5 and 1994.8. The third sub-network was solved in ITRF93 for the epoch 1995.5. The results of these calculations were then transformed to EUREF-89. Due to the transformation method of both mentioned networks, which considers only the horizontal rigid plate motion, it should be reasoned that the vertical component of EUREF-POL network and each sub-network of POLREF network are still for different epochs (1992–1995). The EUREF-POL and POLREF networks points have also determined normal heights in Kronstadt86 system by connecting these networks to the Polish precise levelling network. The normal heights of the Polish levelling network points used in this works, were determined in the third levelling campaign (1974–1982), which was the basis for defining the Kronstadt86 system (*Wyrzykowski, 1988*). This works allowed for determining height anomalies at these points with accuracy initially estimated at cca ± 1.5 cm. However, later analyses indicated a much lower accuracy at the level of ± (3–4) cm (*Kryński, 2007*).

From the early 1990s Polish GPS permanent stations have been included in the EPN network. The number of these stations gradually increased up to the 17 stations that currently operate in the EPN network since 2008 (*Bosy, 2014*). Densification of this network led to the new national permanent GNSS network ASG-EUPOS launched in 2008. Including foreign stations, the ASG-EUPOS network consists of about 120 (about 100 in Poland) GNSS reference stations (*Bosy, 2014*).

In May 1997 the EUVN97 campaign was conducted to integrate the EUREF network with the regional European Mareographic Stations and levelling networks. From these observations 11 points of EUVN network were established at the area of Poland. In 1999 the Polish part of EUVN network was densified by 52 points located at benchmarks of the precise levelling network (*Łyszkowicz et al., 2014*). This network has been developed in ITRF96 for the epoch 1997.4 and transformed to EUREF-89. Since points of the network were also benchmarks of the precise levelling network, their normal heights in the Kronstadt86 system were known.

In the years 2010–2011 a project titled "Integration of the basic geodetic network in the area of Poland with reference stations of the ASG-EUPOS system" was conducted by the Head Office of Geodesy and Cartography in Poland. In this project, eccentric points of ASG-EUPOS points were established and connected to the Polish precise levelling network. A new GNSS observation campaign was also carried out wherein selected points of EUREF-POL, POLREF, EUVN, ASG-EUPOS and its eccentric points were regarded as one network. This allowed for determination of a set of points with precisely designated coordinates in one reference system and epoch covering the entire country. By connecting the eccentric points of ASG-EUPOS network points to the Polish precise levelling network, the normal heights of these points in the Kronstadt86 system were also determined. Thus a large group of points with measured precise GNSS/levelling height anomalies was formed. Selected points from this group (241 points in total) are the basic set of GNSS/levelling test data used in the analyses. Height anomalies determined in these points have an accuracy estimated at ca. ± 1 cm (the author's estimate was made based on the technical report of the project). The coordinates of these points were determined in ITRF2005 for the epoch of 2011.0. The location of these points is presented in Fig. 3a. This set will be later labelled as "ASG2011". Selected points of EUREF-POL and POLREF networks measured in the years 1992–1995 (in total 256 points) form an auxiliary GNSS/levelling set of points that were taken for analyses. These points are shown in Fig. 3b and will be later labelled in short as "POLREF1995". These are the points showing lower (indicated above) accuracy.

33330 gravity points made available by PGI-NRI (The Polish Geological Institute - National Research Institute) were also used in the calculations. These points have gravity accelerations determined in the IGSN71 system and come from a gravity database of more than 800000 points (*Królikowski, 2006*). Gravity measurements were carried out in 1957–1989. Heights of gravity points were determined by spirit levelling with accuracy estimated at cca ± 4 cm. Horizontal coordinates were taken from topographical maps with accuracy at cca ± 50 m (*Królikowski, 2006*). The accuracy of this gravity data is estimated at the level of ± 0.075 mGal (*Kryński, 2007*). These data served to determine gravity disturbances utilised in calculations that refer to the terrain surface. These points cover the whole area of Poland and their mean density is ca. 1 point per 9.3 km^2 (Fig. 3a,b).

To define the volume Ω we used DEM with a resolution of 1000 × 1000 m built on the basis of the GTOPO30 model available on the EROS Center website (basic statistics of DEM: $\max(H) = 2318$ m, $\min(H) = -0.3$ m, st.dev.$(H) = 193$ m). The volume κ was defined on the basis of the Moho depth model for the European plate (*Grad et al., 2009*). The volume Ω was divided into 5250 zones of constant density. A particular zone was a rectangle of the size of 10 × 10 km. Horizontal size and position of single cell of the κ volume corresponded to the appropriate zone of the Ω volume so, in total 10500 constant densities were determined. The horizontal borders of the volumes Ω and κ are the borders of Fig. 3a,b.

In the conducted analyses the results of which are presented later in this work, we adopted either ASG2011 network points or POLREF1995 network points as the known GNSS/levelling data points in various options. We used only ASG2011 points as the test points, which were the basis used to determine accuracy parameters. The accuracy parameters were determined based on the points situated inside "the inner zone".

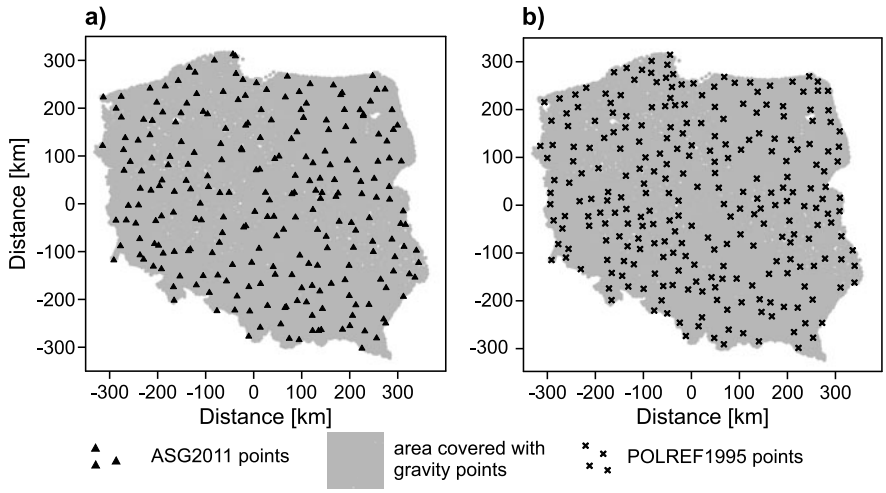

Fig. 3. Location of **a)** ASG2011 and **b)** POLREF1995 points. The border of the area covered with gravity data is the same as the border of Poland.

Considering the two criteria indicated above (location inside the area defined by known GNSS/levelling points and minimum distance from the border of the area covered with gravity data), the border of the inner zone was roughly defined (Fig. 4). This zone includes 199 points of the ASG2011 set. The remaining 42 points lie in the outer zone.

All calculations were done in the local Cartesian coordinate system X, Y, Z, whose origin is in the point φ=52°, λ = 19°.

4. RESULTS OF CALCULATIONS

Calculations were carried out for three research tasks that referred to the estimation of the accuracy of the GGI method. The first task was to estimate the method accuracy parameters using various sets of GNSS/levelling points and various global geopotential models. The second task was to analyse the influence of GNSS/levelling data and gravity data accuracy on the accuracy of the output quasigeoid model. The third task was to assess the influence of the resolution of the global geopotential model on the modelling accuracy.

Accuracy characteristics in all of the calculations were determined in three stages:

1. Building a local quasigeoid model using the GGI method based on gravity data, a set of GNSS/levelling points treated as known points and a selected, global geopotential model.
2. Determination in the test points the differences $\Delta\zeta = \zeta_{\mathrm{GNSS/lev.}} - \zeta_{\mathrm{MOD}}$ between height anomalies that were measured ($\zeta_{\mathrm{GNSS/lev.}}$) and established from the model (ζ_{MOD}).

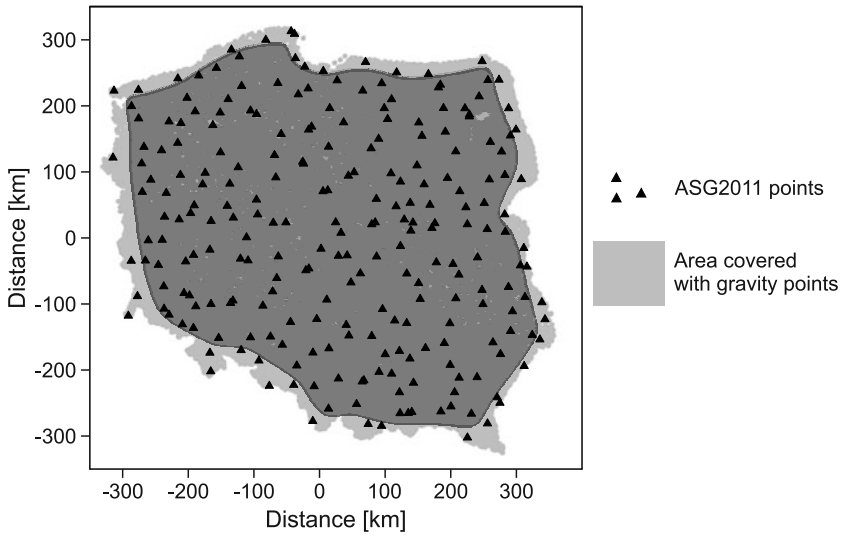

Fig. 4. Inner zone - shaded area. Accuracy parameters were determined based on ASG2011 points located in this zone.

3. Calculation of the basic accuracy characteristics of the model on the basis of differences $\Delta\zeta$. The extreme values of differences $\Delta\zeta$ (minimum and maximum) and a standard deviation of these differences were selected as the accuracy characteristics.

4.1. Estimation of the accuracy parameters of the GGI method

In calculations we used four global geopotential models: EGM96 (*Lemoine et al., 1998*), EGM08, EIGEN-6C2 (*Förste et al., 2012*) and TUMGOCE02S (*Yi, 2012; Yi et al., 2012*). Calculation results are presented in Table 1.

The results presented in Table 1 were divided into two parts due to the use of different sets of known GNSS/levelling points. The first part (first four rows in Table 1) constitutes scenarios where both known and test points come from the same ASG2011 set, which features the high accuracy of the measured height anomalies. In order to determine the accuracy parameters, the LOO (Leave One Out) technique, which is a type of cross validation technique, was used. A series of 199 calculations were carried out for each calculation scenario that used a different global geopotential model. In each series, one point from the ASG2011 set, located in the inner zone, was treated as the test point while the remaining 240 points comprised the set of known points (42 points located in the outer zone were always treated as known points). In this way, differences $\Delta\zeta$ for all 199 points located in the inner zone were obtained. They were later used to calculate the statistics presented in Table 1.

Table 1. Basic accuracy parameters of the GGI method determined on the basis of differences $\Delta\zeta = \zeta_{\text{GNSS/lev.}} - \zeta_{\text{MOD}}$ of the height anomalies measured ($\zeta_{\text{GNSS/lev.}}$) and determined from the model (ζ_{MOD}) in test points. $\Delta\zeta^* = \Delta\zeta - t$ are differences after removing the linear trend in the form $t(X,Y) = a_0 + a_1 X + a_2 Y$. σ: standard deviation. GGM: global geopotential model.

GNSS/levelling Points		GGM		$\Delta\zeta$			$\Delta\zeta^*$		
Data	Test	Name	Max. Degree/ Order	*min* [cm]	*max* [cm]	σ [cm]	*min* [cm]	*max* [cm]	σ [cm]
ASG2011	ASG2011	EGM96	360 360	–2.9	4.0	1.2	---	---	---
ASG2011	ASG2011	EGM08	2190 2159	–3.4	3.4	1.2	---	---	---
ASG2011	ASG2011	EIGEN-6c2	1949 1949	–2.9	3.5	1.2	---	---	---
ASG2011	ASG2011	TUMGOCE02S	230 230	–2.8	4.0	1.2	---	---	---
POLREF1995	ASG2011	EGM08	2190 2159	1.6	13.0	2.1	–4.4	3.4	1.2

In the second part (Row 5 in Table 1), an additional calculation was done, where POLREF1995 points were used as known points. These are the points that feature a lower accuracy of measured height anomalies. 199 ASG2011 points located in the inner zone were adopted as test points. Because the geodetic coordinates (φ, λ, h) of both sets used in the calculations refer to different systems and epochs, the values $\Delta\zeta$ also include differences of height anomalies caused by different systems and epochs. Therefore, in Table 1 we may also find accuracy parameters determined on the basis of $\Delta\zeta^*$. These values were established assuming that the influence of various systems and epochs of known and test GNSS/levelling points, on the determined height anomalies can be expressed as a linear trend: $t(X,Y) = a_0 + a_1 X + a_2 Y$. Trend parameters were determined using the least squares method and the values $\Delta\zeta^*$ in test points were calculated from the equation $\Delta\zeta^* = \Delta\zeta - t$.

Based on the outcomes of the calculations presented above, a very high accuracy of the derived quasigeoid models needs to be emphasised. Irrespective of the global geopotential model used in the calculations, this accuracy was estimated to be at a level of ± 1.2 cm (i.e. the standard deviation of differences $\Delta\zeta$) and is close to the declared accuracy of the measured GNSS/levelling height anomalies in the test points. It is important to note that the global geopotential models that were used have various accuracies and resolutions and the TUMGOCE02S model was developed only on the basis of satellite data.

The use of lower accuracy points (POLREF1995) as the known GNSS/levelling points did not significantly decrease the accuracy of the model being determined. However, it should be noted that accuracy at a level of ± 1.2 cm was achieved after removing the linear trend.

4.2. Analysis of the influence of GNSS/levelling and gravity data accuracy on the accuracy of the GGI method

Test calculations were conducted using ASG2011 points. The set of these points was divided into two groups (Fig. 5). The first group consisted of 131 points located in the inner zone. These points were considered as the test points. The remaining points constituted the set of known points (110 points in total). In calculations we used volumes Ω and κ defined in the same way as before and the same set of gravity data.

In order to analyse the influence of GNSS/levelling and gravity data accuracy on the quasigeoid model accuracy, the measured height anomalies of the known points and gravity disturbances used in the calculations were disturbed with normal distribution noise, with an expected value approaching zero and the projected standard deviation $\sigma_{\zeta d}$ for height anomalies and $\sigma_{\delta g d}$ for gravity disturbances. Based on standard deviations $\sigma_{\zeta d}$ and $\sigma_{\delta g d}$ and the initial errors of GNSS/levelling data ($m_{\text{GNSS/lev.}}$) and gravity data (m_g), the errors of height anomalies m_ζ and gravity disturbances $m_{\delta g}$ adopted for analyses may be estimated. According to the covariance propagation law we can write:

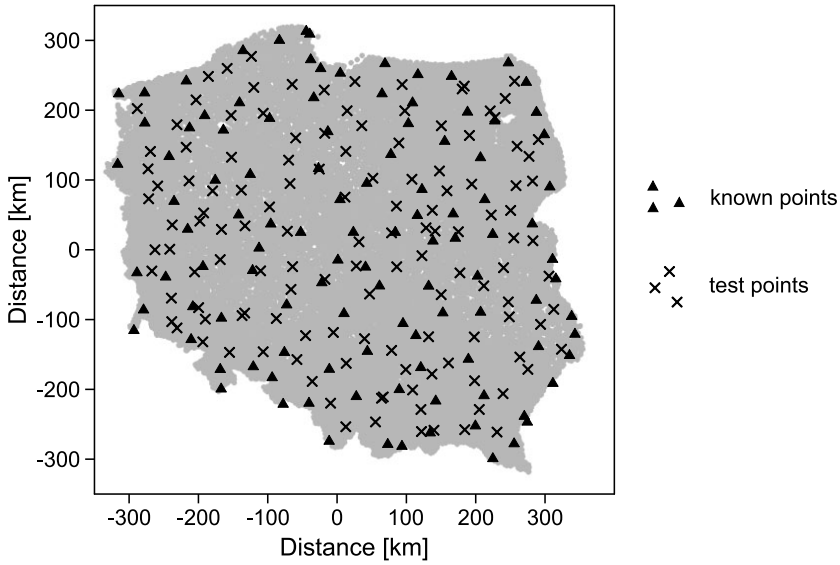

Fig. 5. Location of known and test GNSS/levelling points used in the analyses. Grey area represents the area covered with gravity points.

Table 2. Standard deviation of disturbing noise of height anomalies and gravity disturbances ($\sigma_{\zeta d}$ and $\sigma_{\delta g d}$, respectively) and the corresponding estimated errors m_ζ and $m_{\delta g}$ used in calculations.

$\sigma_{\zeta d}$ [cm]	0.0	0.5	1.0	1.5	2.0	2.5	3.0
m_ζ [cm]	1.0	1.1	1.4	1.8	2.2	2.7	3.2
$\sigma_{\delta g d}$ [mGal]	0.0	0.5	1.0	1.5	2.0	2.5	3.0
$m_{\delta g}$ [mGal]	0.1	0.5	1.0	1.5	2.0	2.5	3.0

$$m_\zeta = \sqrt{\sigma_{\zeta d}^2 + m_{\text{GNSS/lev.}}^2} \quad \text{and} \quad m_{\delta g} = \sqrt{\sigma_{\delta g d}^2 + m_g^2} \ .$$

The errors m_ζ and $m_{\delta g}$ estimated this way and the standard deviations $\sigma_{\zeta d}$ and $\sigma_{\delta g d}$ adopted for analyses are presented in Table 2. In order to calculate the errors m_ζ and $m_{\delta g}$, we assumed that the initial error of GNSS/levelling data was $m_{\text{GNSS/lev}} = \pm 1$ cm and the initial error of gravity was $m_g = \pm 0.075$ mGal (*Kryński, 2007*).

By disturbing the input data, seven sets of known GNSS/levelling points and seven sets of gravity data were derived. For each set of the known GNSS/levelling points, a series of seven test calculations were done, using a different set of gravity data each time. In each calculation series, a standard deviation $\sigma_{\Delta\zeta}$ of differences $\Delta\zeta = \zeta_{\text{GNSS/lev.}} - \zeta_{\text{MOD}}$ was determined based on the set of 131 test points. These standard deviations were used to draw a map of isolines of standard deviations $\sigma_{\Delta\zeta}$, which is presented in Fig. 6. In calculations we used the EGM08 global geopotential model using the RCR technique.

The lightest area in Fig. 6 is the area that corresponds to the quasigeoid model of the highest accuracy at the level of maximum accuracies achieved in previous analyses (approx. ± 1.2 cm). Taking the border of this area into account, one may indicate maximum errors of height anomalies m_ζ and gravity disturbances $m_{\delta g}$, which do not significantly decrease the accuracy of the quasigeoid model. These maximum quantities may be given in two pairs: $m_\zeta < \pm 2$ cm while keeping $m_{\delta g} < \pm 1.3$ mGal and $m_\zeta < \pm 1.2$ cm while keeping $m_{\delta g} < \pm 2.0$ mGal. It is important to note that the indicated limits of the errors are approximate.

4.3. Analysis of relations between the resolution of the global geopotential model used in calculations and the accuracy of the GGI method

Analysis of relations between the resolution of the global geopotential model and the accuracy of the GGI method were performed using the same sets of GNSS/levelling and gravity data as those used in Section 4.2., as well as the EGM08. Calculations were

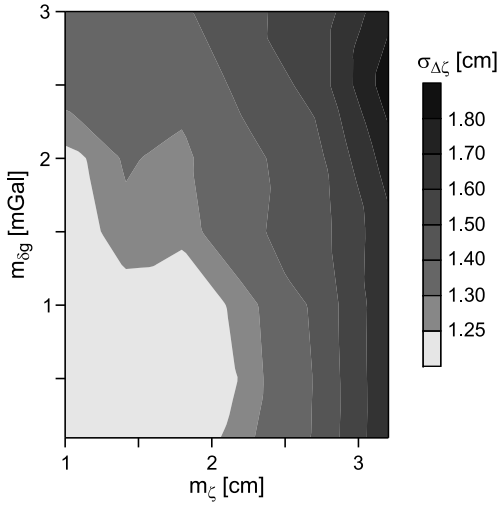

Fig. 6. Values of the standard deviation $\sigma_{\Delta\zeta}$ of differences $\Delta\zeta = \zeta_{\text{GNSS/lev.}} - \zeta_{\text{MOD}}$ as functions of errors of height anomalies m_ζ and of gravity disturbances $m_{\delta g}$.

carried out using the expansion of the global model for 16 different values of the degree N_{max}, which changes in the range from 10 to 2190. Hence, calculations were done for 16 scenarios using a different number of EGM08 coefficients. In each scenario, the differences $\Delta\zeta = \zeta_{\text{GNSS/lev.}} - \zeta_{\text{MOD}}$ were determined for GNSS/levelling test points. These differences were used to estimate the model accuracy in the same way as was done before. Fig. 6 presents the relationship between values N_{max} and the standard deviations of differences $\Delta\zeta$.

While analysing Fig. 7 we must note a very high accuracy of the quasigeoid model, which was determined using very low N_{max}. Only for $N_{max} = 90$ did the standard deviation $\sigma_{\Delta\zeta}$ come to ± 1.25 cm, and it did not exceed ± 1.4 cm for the lower values N_{max}. Similar modelling results were obtained in Section 4.1., where the TUMGOCE02S model was used in the calculations. This suggests that in order to achieve very high accuracies of the quasigeoid model with the GGI method, calculations can be done using low-resolution global geopotential models, built only from satellite observations.

The part of the graph in Fig. 7 for $1600 < N_{max} < 2190$ has an unexpected and surprising course. One can notice a distinct increase of the value $\sigma_{\Delta\zeta}$ (decrease of the model accuracy), which reaches its maximum at $N_{max} \cong 2000$, and a rapid decrease of these values to the level of ca. ± 1.2 cm for $N_{max} = 2190$. To explain the appearance of the graph, the accuracy of the EGM08 model was evaluated for the values N_{max}, which had been used before. Based on 131 GNSS/levelling test points and 33330 gravity points, the

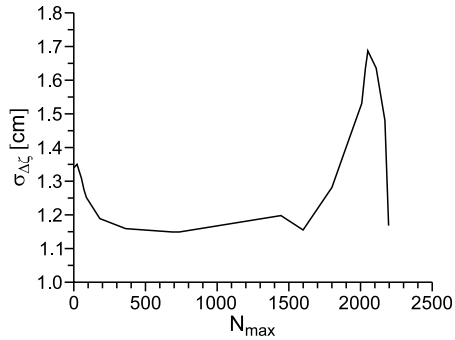

Fig. 7. Values of the standard deviation $\sigma_{\Delta\zeta}$ of differences $\Delta\zeta = \zeta_{\text{GNSS/lev.}} - \zeta_{\text{MOD}}$ as function of the degree N_{max} of coefficients of the EGM08 used in calculations.

differences of height anomalies $\Delta\zeta_N = \zeta_{\text{GNSS/lev.}} - \zeta_{N_{max}}$ and gravity disturbances $\Delta\delta g_N = \delta g - \delta g_{N_{max}}$ as well as the standard deviation of these differences ($\sigma_{\Delta\zeta_N}$ and $\sigma_{\Delta\delta g_N}$, respectively) were determined. In the above equations the value δg stands for the gravity disturbance in the survey point (value determined on the basis of measurements), while $\zeta_{N_{max}}$ and $\delta g_{N_{max}}$ are height anomalies and gravity disturbances determined from the EGM08 truncated to the degree N_{max}.

The graphs of standard deviations $\sigma_{\Delta\zeta_N}$ and $\sigma_{\Delta\delta g_N}$ as functions of the N_{max} degree are presented in Fig. 8.

In addition, for a small part of central Poland ($51.5° \le \varphi \le 52.5°$, $18° \le \lambda \le 20°$), dense grid ($\Delta\varphi = 0.01°$, $\Delta\lambda = 0.02°$) of the $\zeta_{N_{max}}$ and $\delta g_{N_{max}}$ values ($N_{max} \in \{1000, 1600, 2000, 2100, 2190\}$) were determined. Because the changes in height anomalies ($\zeta_{N_{max}}$) were very small in relation to their values, a linear trend:

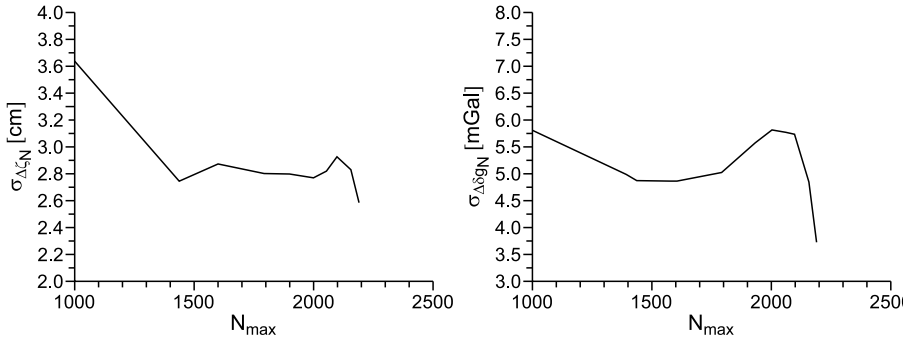

Fig. 8. Values of the standard deviations $\sigma_{\Delta\zeta_N}$ and $\sigma_{\Delta\delta g_N}$ as functions of the degree N_{max} of coefficients of the EGM08 used in calculations.

$t_{N_{max}}(\varphi, \lambda) = a_0 + a_1\varphi + a_2\lambda$ for each set of $\zeta_{N_{max}}$ was estimated by least square method. Subsequently residual height anomalies $\delta\zeta_{N_{max}} = \zeta_{N_{max}} - t_{N_{max}}$ were determined. Contour maps of the values $\delta g_{N_{max}}$ and $\delta\zeta_{N_{max}}$ are presented in Fig. 9.

Let us trace the course of contour lines on the maps presented in Fig. 9. Of course, we do not know the proper course of the lines. Note, however, that the higher resolution of the global model (bigger N_{max}) means a more detailed representation of the actual gravity field. Therefore, we can expect that the least complicated course of contour lines will be visible on the maps for $N_{max} = 1000$ and the most complicated for $N_{max} = 2190$. In Fig. 9 this desired effect is not seen. Relying only on visual assessment, it can be seen that the complexity of the course of contour lines significantly increases from $N_{max} = 1600$ to $N_{max} = 2100$ and clearly decreases for $N_{max} = 2190$. This is particularly noticeable for gravity disturbances. This unexpected course of contour lines corresponds to the graphs of standard deviations $\sigma_{\Delta\zeta_N}$ and $\sigma_{\Delta\delta g_N}$ presented in Fig. 8. There is no expected decrease in the values of $\sigma_{\Delta\zeta_N}$ and $\sigma_{\Delta\delta g_N}$ starting from $N_{max} = 1600$. It can also be distinctly seen an increase in its values near $N_{max} \cong 2100$. The highest determined value $\sigma_{\Delta\delta g_N} = 5.8$ mGal in this area corresponds to the value $N_{max} = 2000$, and the highest value $\sigma_{\Delta\zeta_N} = 2.9$ cm corresponds to the value $N_{max} = 2100$. In both cases the values of these statistics decrease rapidly and reach the minimum for $N_{max} = 2190$. Presented, unexpected behaviour of the EGM08 also explains the course of the graph presented in Fig. 7.

The above analyses indicate that this global geopotential model, the best so far, should be used with all coefficients up to the degree $N_{max} = 2190$ (certainly in the area of Poland), which obviously is a common practice.

5. CONCLUSIONS

Summarising the analyses presented above, we must indicate in particular a very high accuracy of the obtained quasigeoid models. For the global geopotential models used in the calculations, the standard deviation of differences $\Delta\zeta = \zeta_{\text{GNSS/lev.}} - \zeta_{\text{MOD}}$ is at the level of ± 1.2 cm. It must be emphasised that one of the utilised GMs was the TUMGOCE02S model developed on the basis of satellite data only. Such high accuracies were also achieved using the coefficients of the EGM08 to the degree $N_{max} = 90$ only. This suggests that this modelling method may be effectively used in the areas where the surface gravity data were not used to build global geopotential models. Although the achieved accuracy of the models developed using the GGI method are higher than the accuracy of the previous geoid and quasigeoid models developed for the area of Poland, this does not explicitly prove the higher accuracy of this method. This is due to the use of more accurate, previously unavailable GNSS/levelling data.

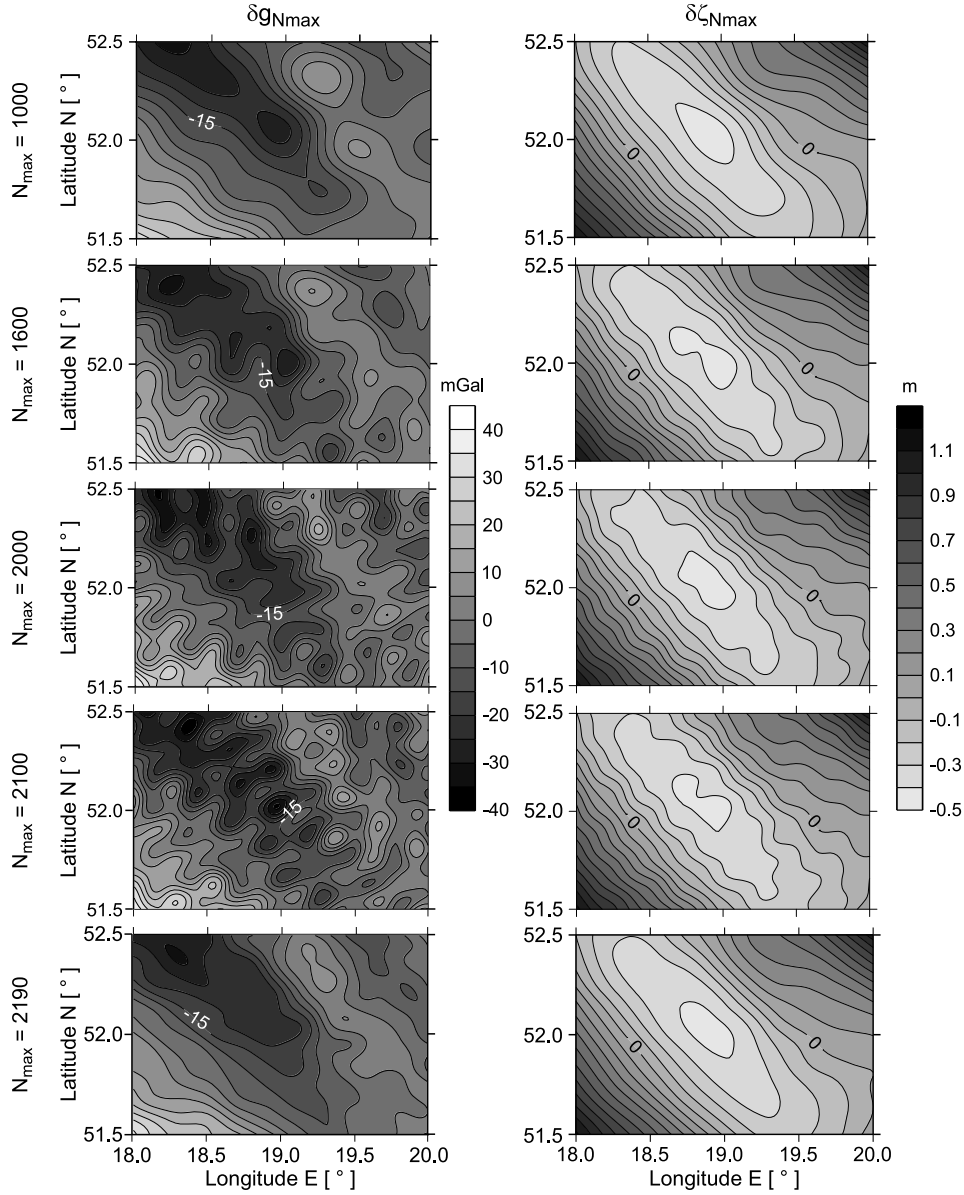

Fig. 9. Contour maps of gravity disturbances $\delta g_{N_{max}}$ (left column) and of residuals height anomalies $\delta\zeta_{N_{max}}$ (right column) determined for different degree values N_{max} from EGM08, for the central part of Poland.

As a result of the analyses we also established accuracy requirements with respect to GNSS/levelling and gravity data. The determined errors of these data should not exceed ± 2 cm for GNSS/levelling height anomalies and ± 1.3 mGal for gravity data. Gravity data accuracies should be even slightly lower ($m_{\delta g} < \pm 2.0$ mGal). However, this requires slightly more accurate GNSS/levelling height anomalies ($m_{\zeta} < \pm 1.2$ cm).

Analyses referring to the EGM08 demonstrated that for geoid/quasigeoid modelling that is based on this model, all of its coefficients up to the degree $N_{max} = 2190$ should be used.

References

Blakely R.J., 1995. *Potential Theory in Gravity and Magnetic Applications*. Cambridge University Press, Cambridge, U.K.

Bosy J., 2014. Global, regional and national geodetic reference frames for geodesy and geodynamics. *Pure Appl. Geophys.*, **171**, 783–808, DOI: 10.1007/s00024-013-0676-8.

Förste C., Bruinsma S. L., Flechtner F., Marty J.-C., Lemoine J.-M., Eahle C., Abrikosov O., Neumayer H., Biancale R., Barthelmes F., Balmino G., 2012. A preliminary upeate of the eirect approach GOCE Processing ane a new release of EIGEN-6C. Presented at the AGU Fall Meeting, 3–7 December 2012, San Francisco, Abstract No. G31B-0923 (http://icgem.gfz-potsdam.de/ICGEM/documents/Foerste-et-al-AGU_2012.pdf).

Godah W., Szelachowska M. and Kryński J., 2014. Accuracy assessment of GOCE-based geopotential models and their use for modelling the gravimetric quasigeoid - a case study for Poland. *Geodesy and Cartography*, **63**, 3–24.

Grad M., Tiira T. and ESC Working Group, 2009. The Moho depth map of the European Plate. *Geophys. J. Int.*, **176**, 279–292, DOI: 10.1111/j.1365-246X.2008.03919.x.

Królikowski C. 2006, Gravity survey at the territory of Poland - its value and importance to the Earth sciences. *Bull. Pol. Geol. Inst.*, **420**, 3–104 (in Polish with English summary).

Krynski J. and Kloch-Główka G., 2009. Evaluation of the performance of the new EGM08 global geopotential model over Poland. *Geoinformation Issues*, **1**, 7–17.

Kryński J., 2007. *Precise Quasigeoid Modelling In Poland - Results And Accuracy Estimation*. Monographic Sseries No 13. Institute of Geodesy and Cartography, Warsaw, Poland (in Polish).

Lemoine F.G., Kenyon S.C., Factor J.K., Trimmer R.G., Pavlis N.K., Chinn D.S., Cox C.M., Klosko S.M., Luthcke S.B., Torrence M.H., Wang Y.M., Williamson R.G., Pavlis E.C., Rapp R.H. and Olson T.R., 1998. *The Development of the Joint NASA GSFC and the National Imagery and Mapping Agency (NIMA) Geopotential Model EGM96*. NASA Technical Report NASA/TP-1996/8-206861, NASA, Greenbelt, Maryland, USA.

Li Y. and Oldenburg D.W., 1998. 3-D inversion of gravity data. *Geophysics*, **63**, 109–119.

Łyszkowicz A. and Forsberg R., 1995. Gravimetric geoid for Poland area using spherical FFT. *IAG Bulletin d'Information No 77*, *IGES Bulletin No 4*, Special Issue, 153–161.

Łyszkowicz A., 2000. Improvement of the quasigeoid model in Poland by GPS and levelling data. *Artif. Satell. J. Planet. Geodesy*, **35**, 3–8.

Łyszkowicz A., 2010. Quasigeoid for the area of Poland computed by least squares collocation. *Techn. Sci.*, No 13, 147–163 9 http://www.uwm.edu.pl/wnt/technicalsc/tech_13/B14.pdf).

Łyszkowicz A., 2012. Geoid in the area of Poland in author's investigations. *Techn. Sci.*, No 15, 49–64 (http://www.uwm.edu.pl/wnt/technicalsc/tech_15_1/B04.pdf).

Łyszkowicz A., Kuczyńska-Siehień J. and Biryło M., 2014. Preliminary unification of Kronsztadt86 local vertical datum with global vertical datum. *Reports on Geodesy and Geoinformatics*, **97**, 103–111.

Nagy D., 1966. The gravitational attraction of right angular prism. *Geophysics*, **31**, 362–371.

Nagy D., Papp G. and Benedek J., 2001. The gravitational potential and its derivatives for the prism. *J. Geodesy*, **74**, 552–560

Pavlis N.K., Holmes S.A., Kenyon S.C. and Factor J.K., 2012. The development and evaluation of the Earth Gravitational Model 2008 (EGM2008). *J. Geophys. Res.*, **117**, B04406, DOI: 10.1029/2011JB008916.

Pażus R., Osada E. and Olejnik S., 2002. The levelling geoid 2001. *Magazyn Geoinformacyjny Geodeta*, No 5(84) (in Polish).

Trojanowicz M., 2007. Local modelling of quasi-geoid heights on the strength of unreduced gravity and GPS/leveling data, with simultaneous estimation of topographic masses density distribution. *Electron. J. Pol. Agric. Univ.*, **10**(4) (http://www.ejpau.media.pl/articles /volume10/issue4/art-35.pdf).

Trojanowicz M., 2012a. Local modelling of quasigeoid heights with the use of the gravity inverse method - case study for the area of Poland**.** *Acta Geodyn. Geomater.*, **9**, 5–18.

Trojanowicz M., 2012b. Local quasigeoid modelling using gravity data inversion technique - analysis of fixed coefficients of density model weighting matrix. *Acta Geodyn. Geomater.*, **9,** 269–281.

Trojanowicz M., 2015. Estimation of optimal quantitative parameters of selected input data used in local quasigeoid modelling by the GGI method. *J. Spat. Sci.*, **60**, 167–178, DOI: 10.1080/14498596.2014.924442.

Wyrzykowski T., 1988. *Monograph on Domestic 1st Class Precise Levelling Networks*. Institute of Geodesy and Cartography, Warsaw, Poland (in Polish).

Yi W., 2012. An alternative computation of a gravity field model from GOCE. *Adv. Space Res.*, **50**, 371–384.

Yi W., Rummel R., Gruber T., 2013. Gravity field contribution analysis of GOCE gravitational gradient components. *Stud. Geophys. Geod.*, **57**, 174–202.

Zielinski J.B., Jaworski L., Zdunek R., Engelhardt G., Seeger H. and Töppe F., 1993. EUREF-POL 1992 Observation Campaign and Data Processing. *Report on the Symposium of the IAG Subcommission for Europe (EUREF) Held in Budapest, Hungary, 17-19 May 1993*. EUREF Publication No 2, Veröffentlichungen der Bayerischen Kommission für die Internationale Erdmessung der Bayerischen Akademie der Wissenschaften, Astronomich-Geodätische Arbeiten, München 1993, Heft Nr. 53, 92–102.

Zieliński J.B., Łyszkowicz A., Jaworski L., Świątek A. and Zdunek R. 1998. POLREF-96 the new geodetic reference frame for Poland. In: Brunner F.K. (Ed.), *Advances in Positioning and Reference Frames*. International Association of Geodesy Symposia **118**, Springer-Verlag, Berlin, Heidelberg, Germany.